JOURNAL OF GUIDANCE, CONTROL, AND DYNAMICS
Vol. 30, No. 3, May–June 2007

Adaptive Variable Structure and Commanding Shaped Vibration Control of Flexible Spacecraft

Qinglei Hu*
Harbin Institute of Technology, 150001 Harbin, People's Republic of China
Peng Shi†
University of Glamorgan, Pontypridd, CF37 1DL, United Kingdom
and
Huijun Gao‡
University of Alberta, Edmonton, Alberta T6G 2V4, Canada

DOI: 10.2514/1.24441

In this paper, a new approach for vibration control of flexible spacecraft during attitude maneuvering is proposed. This control strategy integrates the command input shaping and the technique of dynamic variable structure output feedback control. More precisely, the input shaper is implemented outside of the feedback loop, which is designed for the reference model to achieve the exact elimination of residual vibration by modifying the existing command; whereas for the feedback loop, the controller is designed to make the closed-loop system follow the reference model with input shaper and eliminate the residual vibrations in the presence of parametric uncertainty and external disturbances. An attractive feature of this proposed dynamic variable structure output feedback control algorithm is that the parametric uncertainties of the system are not necessarily to satisfy the so-called matching condition or invariance conditions, provided that certain bounds are known. Furthermore, an adaptive version of the proposed controller is achieved through releasing the limitation of knowing the bounds of the uncertainties and perturbations in advance. The adaptive control law results in substantially simpler stability analysis and improves overall response. Compared with conventional methods, the developed control scheme guarantees not only the stability of the closed-loop system, but also yields better performance and robustness in the presence of parametric uncertainties and external disturbance. Simulation results are presented for the spacecraft model to show the effectiveness of the proposed control techniques.

I. Introduction

MODERN spacecraft often employs large, complex, and lightweight structures such as solar arrays to achieve increased functionality at a reduced launch cost and provide sustainable energy during space flight. The combination of large and lightweight design results in these space structures being extremely flexible and having low-frequency fundamental vibration modes. These modes might be excited in a variety of tasks such as slewing and pointing maneuvers. To effectively suppress the induced vibrations poses a challenging task for the spacecraft designers.

Active control techniques have been increasingly used as the solutions for flexible spacecraft to achieve the degree of vibration suppression for required precision pointing. One special feedforward control strategy, known as input shaping, has been studied widely since its first appearance [1,2] for possessing the advantages of simplicity and effectiveness, because no additional sensor and actuator are required. With this method, an input command is convolved with a sequence of impulses, called an input shaper, to produce a shaped command that causes less vibration than the original unshaped command. Many control schemes were successfully implemented by employing the input-shaping technique. Singhose et al. [3] studied an input-shaping controller for slewing a flexible spacecraft. Banerjee and Singhose [4] proposed the application of input shaping for vibration reduction of flexible spacecraft following momentum damping with/without slewing. Hillsley and Yurkovich [5,6] applied input shaping to large angle movements of a two-link robot, switching to feedback control when approaching the desired position. Using the pulse width/pulse frequency modulation technique, Song et al. [7] considered the application of input shaping for vibration reduction of a flexible spacecraft. Modified input shaping was presented by Shan et al. [8] for multimode vibration suppression of a rotating single-link flexible manipulator. A nonlinear input-shaping technique was presented by Gorinevsky and Vukovich [9] for the flexible spacecraft reorientation maneuver. An adaptive input shaper providing robustness to parameter uncertainties by tuning the shaper to the flexible mode frequencies was explored in [10]; whereas, in [11], the experimental testing of command shaping techniques on a flexible link manipulator was also reported. In addition, Hu and Ma [12] proposed a component control method: component synthesis vibration suppression [13] combined with positive position feedback [14] for flexible spacecraft attitude control, in which a basic proportional-derivative (PD) controller is used for an attitude control subsystem, and the component method is implemented for actively suppressing the vibration of the flexible structure.

On the other hand, in the realistic environment, the knowledge about system parameters such as inertia matrix and modal frequencies is usually unknown (or partially unknown). And various disturbances, including gravitational torque, aerodynamic torque, etc. are also presented. Therefore, disturbance rejection control strategies that are also robust to parametric uncertainty are of great interest in spacecraft applications. Variable structure control (VSC) [15–17] is an effective approach to deal with parametric uncertainties and external disturbances for dynamic systems due to its simplicity and effectiveness as well as its robustness. A tutorial and survey on variable structure control can be found in [16]. A comprehensive guide on sliding mode control for control engineers was given in [17]. VSC is also very interesting to the people in the field of spacecraft attitude control research [18–21] due to its fast dynamic

Received 5 April 2006; revision received 21 August 2006; accepted for publication 22 August 2006.

*Department of Control Science and Engineering.
†School of Advanced Technology.
‡Department of Electrical and Computer Engineering.

control, global asymptotic stability, and invariability for interference perturbation. However, in these studies, it is usually assumed that the spacecraft is rigid and no flexible mode actions are considered. The approaches applied to the rigid model need to be properly modified for flexible spacecraft. In particular, for a highly flexible spacecraft model, the flexibility effect may be directly accommodated into the control law. In the past, significant effort has been put into the problem of attitude control of flexible spacecraft [22,23]. However, these control strategies are mostly limited to the systems with full-state feedback. In practical application, a full measurement of state might neither be possible nor feasible. Consequently, the direct output feedback design in the variable structure system is worth investigating. Heck and Ferri [24] proposed a direct output feedback in the variable structure system by choosing a matrix where the system satisfies the reaching condition. Zak and Hui [25] also proposed a static output feedback method. Some important conditions were given on the switching surface design. Yallapragada et al [26] discussed a design method to obtain a controller that satisfies the reaching conditions. The robustness to external disturbances was also examined when the matching conditions were met. Wang and Fan [27] have developed an interesting approach to design a sliding mode output feedback control. Their definition of sliding hyperplanes includes an exponentially decaying term. Effectively, the system starts from being initially on the sliding hyperplanes. However, the issue of robustness to external disturbances was not addressed, and the uncertainties need to satisfy the matching condition. Kwan [28,29] extended the approach by Wang and Fan [27] by eliminating the exponentially decaying term and formulating a time-varying upper bound of states. He has also examined the robustness to mismatched disturbances. However, this disturbance vector has a special structure that may limit its applicability to many systems. Lewis and Sinha [30] addressed the mismatched disturbance issue concerned with output feedback and presented techniques for stability analysis. However, in their effort, this disturbance vector has a special structure that may limit its applicability to many systems, and modeling uncertainty was not considered. Lewis [31] presented a general sliding mode output feedback control methodology that addressed uncertainty in the plant control, and disturbance matrices providing certain bounds are known. Shyu et al. [32] proposed a modified variable structure output feedback control design method by extending the idea of Zak and Hui [25] and Kwan [28,29] for a matched uncertainty system to a class of mismatched uncertain ones.

However, the bound of uncertainty needs to be available to the designer in advance. These bounds are an important clue to the possibility of guaranteed stability of the closed-loop system. Occasionally, due to the complexity of the structure of uncertainties, it is often observed that in most dynamic systems the characteristics of uncertainties and/or nonlinearities of the controlled plant are in general not available or too expensive/difficult to assess. Hence, the boundary values of the perturbations may not be easily obtained, and these difficulties often become a practical problem for the application of VSC. The adaptive approaches may offer a simple and effective tool to solve this problem [33–35]. The advantages of these controllers are that the information of the upper bound of perturbation is not required.

The contribution of this paper lies in the development of control schemes for vibration reduction of flexible spacecraft. This control strategy integrates the command input shaping and the technique of dynamic variable structure output feedback control (DVSOFC) techniques. In this method, the input shaper is implemented outside of the feedback loop, which is designed, and can achieve the exact elimination of residual vibration of the reference model. The amplitudes and instances of the impulses application can be obtained for the natural frequency and damping ratio of the reference model, respectively. In the feedback loop, the DVSOFC technique is employed to make the closed-loop system behave like the reference system with input shaper and suppress the vibration of the flexible structures in the presence of parametric uncertainty and external disturbances. The robustness to the parametric uncertainty and external disturbances is achieved through the proper selection of control gains. The method for determining these gains is given, as well as a breakdown of the components that contribute to the magnitude of these gains. Also, it should be noted that the parametric uncertainties of the system need not satisfy the so-called matching condition or invariance conditions, and only provided certain bounds are known. In addition, the developed variable structure output feedback controller is also expanded through adaptive dynamic variable structure control without the limitation of knowing the bounds of the uncertainties and the perturbations in advance; that is, an adaptive variable structure output feedback controller is proposed. Moreover, this proposed adaptation law solves the problem that the adaptive switching gains of the controller will slowly increase boundlessly due to the fact that the restriction to the sliding surface cannot always be achieved by adding a negative feedback term and guarantees the boundedness of estimated control gains. To study the effectiveness of the controllers, initially a PD control is developed for control of rigid body motion. This is then extended to incorporate the input shaping for control of the vibration of the flexible structure. The performances of the proposed control strategy are assessed in terms of the attitude pointing capability and vibration reduction as compared with the response to the PD control and the extended case. Furthermore, the comparison with the traditional variable structure output feedback control is also conducted. Simulation results for the spacecraft model show precise trajectory control and vibration suppression.

The rest of the paper is as follows: Sec. II presents the model of the spacecraft with symmetric flexible appendages. The principle of input shaping is briefly described in Sec. III. Section IV describes the detailed control algorithm for the flexible spacecraft. Simulation results are presented and analyzed in Sec. V. The paper is concluded in Sec. VI.

II. Mathematical Model of the Spacecraft

The model of a flexible spacecraft under consideration is shown in Fig. 1. The model consists of a rigid central hub, which represents the spacecraft body, and two flexible appendages, which represent antennas, solar arrays, or any other flexible structures. This model is representative of a relatively large class of spacecraft employed for communication, remote sensing, or numerous other applications [36,37]. We define the $OXYZ$ and $oxyz$ as the inertial frame and the frame fixed on the hub, respectively. Denote $w(x, t)$ as the flexible deformation at point x with respect to the oxy frame, and l is the distance of a point chosen on the appendage from the center of the hub.

In this study, the problem of control of rotational motion from the fixed frame $oxyz$ to the inertial frame $OXYZ$ is considered. Let θ

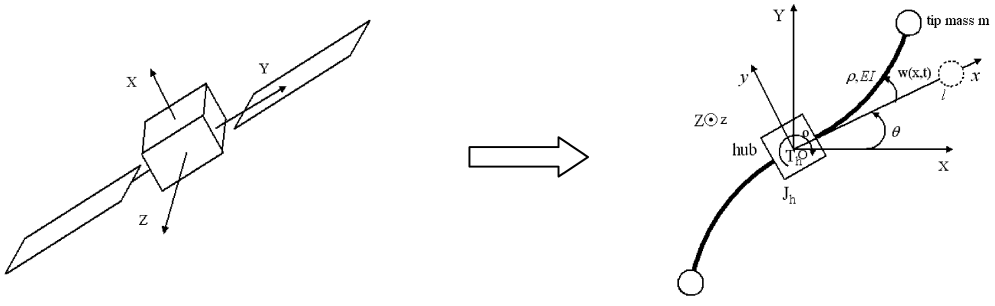

Fig. 1 Spacecraft model with single-axis rotation.

denote the rotation angle which is to be controlled using a torque T_h generating device located at the center of the structure. The flexible appendages tend to vibration due to the coupling effect with the rigid body rotation. It is assumed that the appendages undergo elastic transverse bending only in the orbital plane x–y. They are simplified as flexible beams with tip masses and the frequencies of oscillation are tuned by the tip masses. It is assumed that two solar arrays are identical in geometric and material properties. Under the torque control input only to the center body, the deflection of each solar array should be identical. Namely, the deflection takes place in an antisymmetric fashion.

The equations of motion are derived using the Lagrangian approach. Although the vibration of the appendages is described by partial differential equations, a spatial discretization method is used to obtain a set of ordinary differential equations to describe the motion of the spacecraft. For spatial discretization using the assumed modes method, the transverse elastic deflection of the appendage along y in the $oxyz$ plane is expressed as

$$w(x,t) = \sum_{i=1}^{\bar{N}} \phi_i(x) q_i(t) \tag{1}$$

where $\phi_i(x)$ $(i = 1, 2, \ldots, \bar{N})$ are the chosen admissible functions which satisfy the geometric and physical boundary conditions, and $q_i(t)$ are the generalized coordinates for the flexible deflection. It is assumed here that $\bar{N}$ modes are sufficient for the computation of elastic deformation.

These nonlinear differential equations describing the rotational and elastic dynamics are given by [37]

$$J\ddot{\theta} + M_{\theta q}\ddot{q} = T_h + d \tag{2a}$$

$$M_{\theta q}^T \ddot{\theta} + M_{qq}\ddot{q} + C_{qq}\dot{q} + K_{qq}q = 0 \tag{2b}$$

where $q = [q_1, q_2, \ldots, q_{\bar{N}}]^T$, the element mass, stiffness matrices, and the nonlinear terms are governed by

$$J = J_h + 2\int_b^l \rho x^2 \, \mathrm{d}x + 2m_t l^2$$

$$M_{\theta q} = 2\int_b^l \rho x \phi_i(x) \, \mathrm{d}x + 2m_t l \phi_i(l)$$

$$M_{qq} = 2\int_b^l \rho \phi_i(x)\phi_j(x) \, \mathrm{d}x + 2m_t \phi_i(l)\phi_j(l)$$

$$K_{qq} = 2\int_b^l \underline{E}\underline{I}\phi_i''(x)\phi_j''(x) \, \mathrm{d}x$$

$$C_{qq} = 2\int_b^l \underline{C}\underline{I}\phi_i''(x)\phi_j''(x) \, \mathrm{d}x$$

Here, $\underline{C}$and E are the damping coefficient and modulus of elasticity, respectively, for the appendages and $\underline{I}$ is the sectional area moment of inertia with respect to the appendage bending axis, and $d(t) \in R$ is the external disturbances which belong to $L_2[0, \infty)$ and $\|d(t)\| \le \delta_d$ where δ_d is a known positive constant.

Equation (2) can be written in a compact form as

$$\bar{M}\ddot{\bar{Z}} + \bar{C}\dot{\bar{Z}} + \bar{K}\bar{Z} = \bar{B}[T_h + d(t)] \tag{3}$$

where $\bar{Z} = [\theta, q^T]^T \in R^{\bar{N}+1}$,

$$\bar{M} = \begin{bmatrix} J & M_{\theta q} \\ M_{\theta q}^T & M_{qq} \end{bmatrix}$$

$\bar{C} = \mathrm{diag}\{0, C_{qq}\}$, $\bar{K} = \mathrm{diag}\{0, K_{qq}\}$, $\bar{B} = \begin{bmatrix} 1 \\ 0 \end{bmatrix}$, $\bar{\bar{B}} = \begin{bmatrix} 0 \\ 1 \end{bmatrix}$, and 0 denotes a null vector of appropriate dimension.

The system of $\bar{Z}$ second-order differential equations, Eq. (3) can be transformed into the state-space form

$$\dot{x} = Ax + B\bar{u}(t) + Bd(t) \tag{4}$$

where

$$x = \begin{bmatrix} \bar{Z} \\ \dot{\bar{Z}} \end{bmatrix}$$

$$A = \begin{bmatrix} 0 & I \\ -\bar{M}^{-1}\bar{K} & -\bar{M}^{-1}\bar{C} \end{bmatrix}$$

$$B = \begin{bmatrix} 0 \\ \bar{M}^{-1}\bar{B} \end{bmatrix}$$

$$\bar{u}(t) = T_h$$

Considering the flexible space structure as shown in Fig. 1, the objective of the slew maneuver of this study is a rest-to-rest maneuver from a rest state to another rest state in the shortest time possible. The angle $\theta(t)$ is rotated from the initial state to $\theta_d \in [0, 2\pi]$, for example, setting to 60 deg throughout this study. The sensor output available for the output feedback is hub angle θ and angular rate $\dot{\theta}$. Based on the customary requirements of the flight task of an actual spacecraft, the control scheme should also satisfy the following dominating demands: 1) short transient time, no overshooting or less overshooting, and high precision, and less vibration stirred; 2) strong capability to resist disturbance of vibrations in both the transient process and the steady state.

III. Input Shaping

Input shaping is the technique of convolving a sequence of impulse, an input shaper, with the desired command to a flexible structure so that the "shaped command" results in zero residual vibration. This technique is developed based on linear systems theory. A simple illustration of this technique is shown in Fig. 2. In this figure, the vibration caused by the first impulse can be eliminated by applying an additional impulse of an appropriate amplitude and phase. In this section, some commonly used shapers are reviewed to assist with the design of the shaper for the slew operation of the flexible spacecraft. Relevant research on this subject can be found, for example, see [1,2].

In Fig. 2, the responses (thin solid and dashed lines) caused by two impulses (vertical arrows) are superposed to result in a nonvibratory response (thick line)

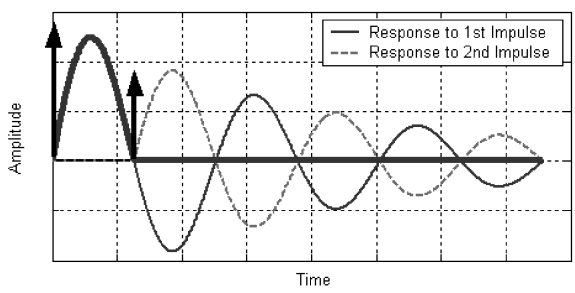

Fig. 2 Vibration cancellation using input shaping.

Consider a linear second-order system (5) having natural frequency ω_n and damping ratio ξ, its response to a sequence of $\tilde{N}$ impulse is described by (6)

$$G(s) = \frac{\omega_n^2}{s^2 + 2\xi\omega_n + \omega_n^2} \tag{5}$$

$$y(t) = \sum_{i=1}^{\tilde{N}} \left\{ \frac{X_i \omega_n}{\sqrt{1-\xi^2}} e^{-\xi\omega_n(t-t_i)} \sin[\omega_n \sqrt{1-\xi^2}(t-t_i)] \right\} \tag{6}$$

where X_i and t_i are the amplitude and the application time of the ith impulse, respectively; these are the parameters to be determined for the input-shaping technique design by using the following constraints, (7a) and (7b), derived from (6)

$$\sum_{i=1}^{\tilde{N}} \left[X_i t_i^q e^{-\xi\omega_n(t_N - t_i)} \sin(t_i \omega_n \sqrt{1-\xi^2}) \right] = 0 \tag{7a}$$

$$\sum_{i=1}^{\tilde{N}} \left[X_i t_i^q e^{-\xi\omega_n(t_N - t_i)} \cos(t_i \omega_n \sqrt{1-\xi^2}) \right] = 0 \tag{7b}$$

where $q = 0, 1, \ldots, \tilde{N} - 2$. The above two constraints were derived from the requirements that the amplitude of $y(t)$ and its derivatives (with respect to ω_n) be made zero for $t > t_{\tilde{N}}$ which imply zero amplitude of vibration after $t_{\tilde{N}}$. In addition, two further constraints need to be added:

$$t_1 = 0 \tag{8a}$$

$$\sum_{i=1}^{\tilde{N}} X_i = 1 \tag{8b}$$

The first constraint (8a) simply reflects the choice of a time origin; the second constraint (8b) reflects the requirement that the total sum of X_i be equal to unity. Note that as $\tilde{N}$ is increased from its minimum number, $\tilde{N} = 2$, the input-shaping technique becomes less sensitive to the estimation error of ω_n and ξ due to system uncertainty [2]. However, the larger $\tilde{N}$ becomes, the larger the time delay becomes due to the input-shaping technique. From the above equations, X_i and t_i are determined as follows:

$$X_j = \frac{\binom{\tilde{N}-1}{j-1} K^{j-1}}{\sum_{i=0}^{\tilde{N}-1} \binom{\tilde{N}-1}{i} K^i} \tag{9a}$$

$$t_i = (j-1)\frac{\pi}{\omega_n \sqrt{1-\xi^2}} \tag{9b}$$

where $K = \exp -(\pi\xi)/(\sqrt{1-\xi^2})$. It is noted that the amplitudes and the instances in (9) depend on the system parameters, that is, the system natural frequency ω_n and the damping ratio ξ.

The input shaper impulse sequences can also be generalized to consider more than one vibration mode, by convolving the impulse sequences for each individual mode with one another. Let the input with $\tilde{N}_j$ $(j = 1, \ldots, n)$ $(n > 1)$ impulses be used in the jth mode. After the necessary convolutions, the input impulse sequences, X_{mult}, can be expressed

$$X_{\text{mult}} = X_{1s} * X_{2s} \cdots * X_{ns} \tag{10}$$

where X_{js} is the impulse sequences of the jth mode of the system with $\tilde{N}_j$ impulses, and * is the convolution operator.

In this manner, for a vibratory system, the described impulse sequence can be convolved to an arbitrary input, to obtain the same vibration-reducing properties of the impulsive input case. However, the major drawback of the input shaping, being open-loop controllers, is its limitation in coping with parameter changes and disturbances to the system. Moreover, this technique requires relatively precise knowledge of the dynamics of the system. If models have parametric uncertainties, system performance will not result in zero residual vibration. Even if several design approaches have been proposed to improve the robustness of input shaping to the damping factors and natural frequencies of the flexible structure [8–10]. It should also be noted that the plant being linear is essential for proving why the input-shaping technique works. Here, the model of the flexible spacecraft considered in Sec. II includes nonlinear terms, such as unstructured uncertainties and the coupling term on the right side of Eq. (4). Therefore, in this paper, the input shaping is applied in conjunction with the VSC for maneuvers of flexible spacecraft. This paper shows preliminary results that indicate such control architecture provides very good performance. The following systematic design procedure will be provided for designing the variable structure controller.

IV. Dynamic Variable Structure Output Feedback /Input-Shaping Control

To improve the robustness and performance of the input-shaping method, a variable structure controller combined with input shaping is presented, as shown in Fig. 3. The impulse shaper is also implemented outside of the feedback loop, but is designed for the reference model and achieves the exact elimination of residual vibration. The amplitudes and instances of the impulse application can be obtained from Eq. (9) with the natural frequency ω_{mn} and the damping ratio ξ_m of the reference model, respectively. Although the feedback controller based on DVSOFC is designed to make the closed-loop system behave like the reference model with a shaper and eliminate the residual vibrations. This is an effective method of implementing input shaping for satisfactory performance and robustness even when parameter variations and external disturbance occur simultaneously in the process.

From Fig. 3, system (4) can be rewritten as

$$\dot{x} = Ax + Bu(t) + Bu_d + Bd(t) \tag{11}$$

Here, the reference model is selected as the nominal system. The combination of the input shaper convolving with the reference model dynamics can be expressed as

$$\dot{x}_m = A_m x_m + B_m u_d \tag{12}$$

where A_m and B_m are the known matrices of the nominal system.

According to the principle of the input-shaping technique, the shaped input u_d can be expressed as

$$u_d = u_{\theta_d} * X_{\text{mult}} \tag{13}$$

Here, u_{θ_d} is the computed torque using the desired trajectory θ_d [38].

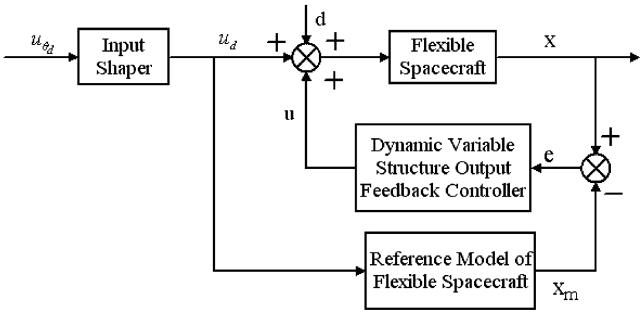

Fig. 3 A block diagram of proposed control method for flexible spacecraft vibration reduction.

Applying the convolution operator, Eq. (13) can be rewritten as

$$u_d = \left(\prod_{j=1}^{n} X_{j,1}\right) u_{\theta_d} + X_{1,2}\left(\prod_{j=2}^{n} X_{j,1}\right) u_{\theta_d}(t - t_{1,2}) + \cdots + \left(\prod_{j=1}^{n} X_{j,\tilde{N}_j}\right) u_{\theta_d}\left(t - \sum_{j=1}^{n} t_{j,\tilde{N}_j}\right) \tag{14}$$

To simplify the notation, Eq. (14) can be written as

$$u_d = \sum_{k=0}^{2n-1} a_k u_{\theta_d}(t - t_k) \tag{15}$$

where

$$a_0 = \prod_{j=1}^{n} X_{j,1}$$

$$a_1 = X_{1,2} \prod_{j=2}^{n} X_{j,1}, \ldots$$

$$a_{2n-1} = \prod_{j=1}^{n} X_{j,\tilde{N}_j}$$

$$t_0 = 0$$

$$t_1 = t_{1,2}, \ldots, t_{2n-1} = \sum_{j=1}^{n} t_{j,\tilde{N}_j}$$

Substituting (15) into Eqs. (12) and (13), the following equations can be obtained:

$$\dot{x} = Ax + Bu(t) + B\left[\sum_{k=0}^{2n-1} a_k u_{\theta_d}(t - t_{dk})\right] + Bd(t) \tag{16}$$

Here the time of the impulse application is assumed to be inaccurate, that is, $t_{dk} \neq t_k$.

$$\dot{x}_m = A_m x_m + B_m\left[\sum_{k=0}^{2n-1} a_k u_{\theta_d}(t - t_k)\right] \tag{17}$$

The parameter variations of the system considered here are defined as follows. The parameter uncertainties of the system ΔA can be expressed as

$$\Delta A = A - A_m \tag{18}$$

It is noted that in this work the uncertainty matrix ΔA does not need to satisfy the so-called matching condition. Here, the input matrix is assumed to satisfy the following condition. However, the uncertainty in the input is assumed to satisfy the matching condition and can be expressed as

$$B = B_m \tag{19}$$

Introducing $e(t) = x(t) - x_m(t)$ into Eqs. (16) and (17), the error dynamics are expressed in terms of the error state vector $e(t)$.

$$\dot{e} = (A_m + \Delta A)e + B_m u + \Delta A x_m + B_m D_f \tag{20}$$

where

$$D_f = \sum_{k=0}^{2n-1} a_k[u_{\theta_d}(t - t_{dk}) - u_{\theta_d}(t - t_k)] + d$$

It is assumed in this study that the attitude angle and angular velocity are measurable, and the elastic modes are unavailable. The measurement available for the controller design can be expressed in the output form as

$$y = Ce \tag{21}$$

where $y \in R^p$ and C is an appropriately dimensioned matrix.

Throughout the remainder of this paper, the following assumptions are taken to be valid:

Assumption 1: The triplet (A_m, B_m, C) is controllable and observable.

Assumption 2: There exist known nonnegative constants k_1, k_2, and k_3 such that the uncertainties ΔA and lumped disturbance D_f are unknown but bounded as

$$\|\Delta A\| \leq k_1, \qquad \|D_f\| \leq k_2 + k_3\|e\| \tag{22}$$

A. Switching Surface and Dynamic Variable Structure Output Feedback Controller Design

Now, the switching surface is defined as [24,25,32]

$$\sigma = Gy = GCx = Se \tag{23}$$

where $G \in R^{m \cdot p}$ is a constant matrix. The matrix G should be selected to satisfy $GC = S$. Conditions were given in [24,25,32] for how to choose S so that $(n - m)$ prescribed nonzero and complex eigenvalues $\{\lambda_1, \lambda_2, \ldots, \lambda_{n-m}\}$ with $\mathrm{Re}(\lambda_j) < 0$ $(j = 1, 2, \ldots, n - m)$ can be assigned.

To simplify the development of the control design scheme, a state transformation $z = Tx$ is applied in the subsequent section. By assumption 1, there always exist matrices $T \in R^{n \cdot (n-m)}$ and $N \in R^{m \cdot n}$ such that $[A_m + B_m N]T = TJ$, where $J \in R^{(n-m)\cdot(n-m)}$ is a freely chosen Jordan matrix which determines the system dynamics restricted to the switching surface. The eigenvalues of J, λ_j, $j = 1, 2, \ldots, n - m$ are the desired eigenvalues in the sliding mode. Let $\lambda_{\max}$ and $\lambda_{\min}$ denote the maximum and minimum eigenvalues of λ_j $j = 1, 2, \ldots, n - m$, respectively. The next assumption will be used in the subsequent section.

Assumption 3: The matrix $[T\ B_m]$ is invertible.

Suppose that the inverse $[T\ B_m]$ has the form $\begin{bmatrix} \bar{T} \\ \bar{B}_m \end{bmatrix}$ where $\bar{T}$ and $\bar{B}_m$ denote the generalized inverse of T and B_m, respectively. Without any loss of generality, selecting $S = \bar{B}_m$ and a transformation matrix $H = \begin{bmatrix} \bar{T} \\ S \end{bmatrix}$ with $H^{-1} = [T\ B_m]$ then system (20), neglecting the term $\Delta A x_m$, can be written by

$$\dot{z} = \bar{T}(A_m + \Delta A)Tz + \bar{T}(A_m + \Delta A)B_m\sigma \tag{24a}$$

$$\dot{\sigma} = S(A_m + \Delta A)Tz + S(A_m + \Delta A)B\sigma + u + D_f \tag{24b}$$

Here, since ΔA is bounded, and $x_m \to 0$ as $t \to \infty$, the term $\Delta A x_m$ in (20) will decay to zero as $t \to \infty$. Hence it will not affect the equilibrium point of the system (24a). In the following, the analysis of system stability in the sliding mode is on the basis of the transformed system (24).

The following two lemmas will be used in the proof of the subsequent main results of Theorem 1.

Lemma 1: Let $\|\Delta A\| \leq k_1$

$$P = \mathrm{diag}\{\lambda_{\min}/\lambda_1, \lambda_{\min}/\lambda_2, \ldots, \lambda_{\min}/\lambda_{n-m}\} \tag{25}$$

If

$$k_1 < -\lambda_{\min}/(\|P\bar{T}\|\,\|T\|) \tag{26}$$

then the mismatched uncertain system (20) in the sliding mode is asymptotically stable.

Lemma 2: Assume $C' \geq 0$, $r(t)$, $h(t)$, and $g(t)$ are nonnegative-valued continuous functions. If

$$r(t) \leq C' + \int_0^t h(\tau)\,\mathrm{d}\tau + \int_0^t g(\tau)\,\mathrm{d}\tau \tag{27}$$

then

$$r(t) \leq C' \exp\{f(t)\} + \int_0^t g(\tau)\exp\{f(t) - f(\tau)\}\,\mathrm{d}\tau \tag{28}$$

where

$$f(t) = \int_0^t h(\tau)\,\mathrm{d}\tau \tag{29}$$

Proof of Lemmas 1 and 2: Omitted for brevity; see, for example, [32] and references therein.

Applying the two lemmas, we can derive the following theorem.

Theorem 1: Consider Eq. (24a)

$$\dot{z} = (J + \bar{T}\Delta A T)z + (\bar{T}A_m B_m + \bar{T}\Delta A B_m)\sigma \tag{30}$$

Then the following two statements hold:

1) $\|\exp(Jt)\| \le k_4 \exp(\lambda_{\max} t)$ for some $k_4 > 0$.

2) $\|z\|$ is bounded by $\eta(t)$ for all time, where $\eta(t)$ is the solution of

$$\dot{\eta}(t) = \lambda\eta(t) + k_4(\|\bar{T}A_m B_m\| + \rho_2)\|\sigma\|, \qquad \eta(0) \ge k_4\|z(0)\| \tag{31}$$

with $\lambda = \lambda_{\max} + k_4\rho_1$.

Proof: The following will give the brief derivation to assist with the design of the variable structure controller later. Because all the eigenvalues of J are real negative, condition 1) holds obviously. See the details in [32]. To see 2), we solve (31) to yield

$$\begin{aligned}\|z(t)\| &\le \|e^{Jt}\|\,\|z(0)\| + \int_0^t \|e^{J(t-\tau)}\|\,\|\bar{T}\Delta A T z(\tau) \\ &\quad + (\bar{T}A_m B_m + \bar{T}\Delta A B_m)\sigma\|\,\mathrm{d}\tau \\ &\le k_4 \exp(\lambda_{\max} t)\|z(0)\| + \int_0^t k_4 \exp(\lambda_{\max}(t-\tau))\|\bar{T}\Delta A T z(\tau) \\ &\quad + (\bar{T}A_m B_m + \bar{T}\Delta A B_m)\sigma\|\,\mathrm{d}\tau \end{aligned} \tag{32}$$

For the above inequality, we multiply the term $\exp(-\lambda_{\max} t)$ to both sides and using (30), then

$$\begin{aligned}\|z(t)\|\exp(-\lambda_{\max} t) &\le k_4\|z(0)\| + \int_0^t k_4 \exp(-\lambda_{\max}\tau)\rho_1\|z(\tau)\|\,\mathrm{d}\tau \\ &\quad + \int_0^t k_4 \exp(-\lambda_{\max}\tau)(\|\bar{T}A_m B_m\| + \rho_2)\|\sigma\|)\,\mathrm{d}\tau \end{aligned} \tag{33}$$

Applying Lemma 2, we can obtain

$$\begin{aligned}\|z(t)\|\exp(-\lambda_{\max} t) &\le k_4\|z(0)\|\exp(k_4\rho_1 t) \\ &\quad + \int_0^t k_4 \exp(-\lambda_{\max}\tau)(\|\bar{T}A_m B_m\| + \rho_2)\|\sigma\|) \\ &\quad \cdot \exp[k_4\rho_1(t-\tau)]\,\mathrm{d}\tau \end{aligned} \tag{34}$$

Shift the term $\exp(-\lambda_{\max} t)$ to the right-hand side for the above inequality, if $\eta(0) \ge k_4\|z\| > 0$, we have

$$\begin{aligned}\|z(t)\| &\le k_4\|z(0)\|\exp[(\lambda_{\max} + k_4\rho_1)t] + \int_0^t k_4 \exp[(\lambda_{\max} \\ &\quad + k_4\rho_1)(t-\tau)](\|\bar{T}A_m B_m\| + \rho_2)\|\sigma\|)\,\mathrm{d}\tau \\ &\le \eta(0)\exp[(\lambda_{\max} + k_4\rho_1)t] + \int_0^t k_4 \exp[(\lambda_{\max} + k_4\rho_1) \\ &\quad \times (t-\tau)](\|\bar{T}A_m B_m\| + \rho_2)\|\sigma\|)\,\mathrm{d}\tau = \eta(t) \end{aligned} \tag{35}$$

where $\eta(t)$ satisfies (31). Hence, we can see that $\eta(t) \ge \|z(t)\|$ for all time, if $\eta(0)$ is sufficiently large.

Once a proper switching surface has been chosen, it is followed by choosing a variable structure control to derive the system trajectory onto the sliding surface. To ensure the occurrence of the sliding motion, the following dynamic variable structure controller is selected to be

$$u = -k_5\sigma - [k_6\eta(t) + k_7]\sigma/\|\sigma\| - \alpha\sigma/\|\sigma\| \tag{36}$$

where $\alpha > 0$ and k_5, k_6, and k_7 are constant gains. It should be pointed out that the controller could use only the output signal. Inspection of Eq. (36) indicates that the control law is time varying due to the $\eta(t)$ and $\sigma(t)$ terms.

Theorem 2: Consider the mismatched uncertain system (20). Under the assumptions 1–3, the dynamic variable structure output feedback control law (36) drives the system to the sliding surface and maintains a sliding motion thereafter if the constant gains satisfy the following conditions:

$$k_5 > \|SA_m B_m\| + k_1\|S\|\,\|B_m\| + k_3\|B_m\| \tag{37a}$$

$$k_6 > \|SA_m T\| + k_1\|S\|\,\|T\| + k_3\|T\| \tag{37b}$$

$$k_7 > k_2 \tag{37c}$$

Proof: Since $e = Tz + B_m\sigma$, using Theorem 2, we have $\|x\| \le \|T\|\eta(t) + \|B_m\|\,\|\sigma\|$. It follows from (24) and assumption 1 that

$$\begin{aligned}\sigma^T\dot{\sigma} &= \sigma^T SA_m Tz + \sigma^T SA_m B_m\sigma + \sigma^T S\Delta A T z + \sigma^T S\Delta A B_m\sigma \\ &\quad + \sigma^T(u + D_f) \le \|SA_m B_m\|\,\|\sigma\|^2 + k_1\|S\|\,\|B_m\|\,\|\sigma\|^2 \\ &\quad + \|SA_m T\|\,\|\sigma\|\eta(t) + k_1\|S\|\,\|T\|\,\|\sigma\|\eta(t) \\ &\quad + [k_2 + k_3(\|T\|\eta(t) + \|B_m\|\,\|\sigma\|)]\|\sigma\| - [\|SA_m B_m\| \\ &\quad + k_1\|S\|\,\|B_m\| + k_3\|B_m\|]\|\sigma\|^2 - [\|SA_m T\| + k_1\|S\|\,\|T\| \\ &\quad + k_3\|T\|]\|\sigma\|\eta(t) - k_2\|\sigma\| - \alpha\|\sigma\| \le -\alpha\|\sigma\| \end{aligned} \tag{38}$$

Then using the controller in (36) with the gain constraint in (37), the inequalities (38) become $\sigma^T\dot{\sigma} \le -\alpha\|\sigma\|$. Hence the state trajectory will reach the switching surface in finite time and stay on it thereafter.

B. Adaptive Dynamic Variable Structure Output Feedback Control Design

In the above section, we have shown how to design a stable system by dynamic variable structure control for the systems with mismatched uncertainty. However, the bounds of the uncertainties/disturbances must be known in advance. In general, this bound is difficult to measure in practical applications; therefore, the bound of the uncertainty is usually chosen large enough to ensure robust stability. However, a large parameter will result in substantial chattering of the control effort. On the other hand, if the bound is chosen too small, the robust stability cannot be guaranteed. To relax the requirement for the bound of uncertainty, an adaptive design method for the robust gain is proposed. Here, we recall the Barbalat lemma [39] in the following. Barbalat lemma will be a tool used in the proof of the subsequent main result of Theorem 3.

Lemma 3: If $g : R \to R$ is uniformly continuous for $t \ge 0$ and if the limit of the integral [39]

$$\lim_{t\to\infty} \int_0^t |g(\tau)|\,\mathrm{d}\tau \tag{39}$$

exists and is finite, then

$$\lim_{t\to\infty} g(t) = 0 \tag{40}$$

Now, the following adaptive dynamics variable structure output feedback control is proposed as

$$u = -k_5\sigma - [k_6\eta(t) + k_7]\sigma/\|\sigma\| - \alpha\sigma/\|\sigma\| \tag{41}$$

where k_j ($j = 5, 6, 7$) are chosen to be

$$k_5 > \|SA_m B_m\| + \hat{k}_1\|S\|\,\|B_m\| + \hat{k}_3\|B_m\| \tag{42a}$$

$$k_6 > \|SA_m T\| + \hat{k}_1\|S\|\,\|T\| + \hat{k}_3\|T\| \tag{42b}$$

$$k_7 > \hat{k}_2 \tag{42c}$$

and $\hat{k}_i$ ($i = 1, 2, 3$) is the estimate of k_i ($i = 1, 2, 3$) and $\hat{k}_i$ ($i = 1, 2, 3$)

can be obtained from the following dynamics:

$$\dot{\hat{k}}_1 = -\mu_1(t)\hat{k}_1 + \frac{1}{p_1}\|S\|\,\|\sigma\|[\|B_m\|\,\|\sigma\| + \|T\|\eta(t)] \tag{43a}$$

$$\dot{\hat{k}}_2 = -\mu_2(t)\hat{k}_2 + \frac{1}{p_2}\|\sigma\| \tag{43b}$$

$$\dot{\hat{k}}_3 = -\mu_3(t)\hat{k}_3 + \frac{1}{p_3}\|\sigma\|[\|B_m\|\,\|\sigma\| + \|T\|\eta(t)] \tag{43c}$$

$$\dot{\mu}_i(t) = -r_i\mu_i(t) \tag{43d}$$

where p_i is positive constant as the adaptive gain, $\mu_i(0) > 0$ and $r_i > 0$ $(i = 1, 2, 3)$. Here, the negative feedback term $-\mu_i(t)\hat{k}_i$ $(i = 1, 2, 3)$ is introduced to solve the problem that the adaptive switching gains of the controller will slowly increase boundlessly due to the fact that the restriction to the sliding surface cannot always be achieved.

Let $\bar{k}_i = k_i - \hat{k}_i$ $(i = 1, 2, 3)$ denote the adaptation error. Because k_i $(i = 1, 2, 3)$ is assumed to be constant, then the following expression remains valid:

$$\dot{\bar{k}}_i = -\dot{\hat{k}}_i \qquad (i = 1, 2, 3) \tag{44}$$

Theorem 3: Consider system (20) under assumptions 1 and 3, if this system is controlled by $u(t) = \tilde{u}(t)$ in (41) with adaptation law (43), then the system trajectory converges to the sliding surface $\sigma(t) = 0$.

Proof: Consider the following Lyapunov function candidate:

$$\tilde{V} = \frac{1}{2}[\|\sigma\|^2 + \bar{k}^T\Gamma\bar{k}] + k^T\Gamma R^{-1}\mu k \tag{45}$$

where $k = [k_1\ k_2\ k_3]^T$, $\bar{k} = [\bar{k}_1\ \bar{k}_2\ \bar{k}_3]^T$, $\Gamma = \mathrm{diag}\{p_1, p_2, p_3\}$, $R = \mathrm{diag}\{r_1, r_2, r_3\}$, $\mu = \mathrm{diag}\{\mu_1, \mu_2, \mu_3\}$, $(\mu k) = [\mu_1 k_1\ \mu_2 k_2\ \mu_3 k_3]^T$. Differentiating $\tilde{V}$ with respect to time t

$$\begin{aligned}
\dot{\tilde{V}} &= \sigma^T\dot{\sigma} + \bar{k}^T\Gamma\dot{\bar{k}} + k^T\Gamma R^{-1}\dot{\mu}k = \sigma^T SA_mTz + \sigma^T SA_mB_m\sigma \\
&\quad + \sigma^T S\Delta ATz + \sigma^T S\Delta AB_m\sigma + \sigma^T(u + D_f) + \bar{k}^T\Gamma\dot{\bar{k}} \\
&\quad + k^T\Gamma R^{-1}\dot{\mu}k \le \|SA_mB_m\|\,\|\sigma\|^2 + k_1\|S\|\,\|B_m\|\,\|\sigma\|^2 \\
&\quad + \|SA_mT\|\,\|\sigma\|\,\|z\| + k_1\|S\|\,\|T\|\,\|\sigma\|\,\|z\| + (k_2 \\
&\quad + k_3\|x\|)\|\sigma\| + \sigma^T\{-\hat{k}_5\sigma - [\hat{k}_6\eta(t) + \hat{k}_7]\sigma/\|\sigma\| - \alpha\sigma/\|\sigma\|\} \\
&\quad + \bar{k}^T\Gamma\dot{\bar{k}} + k^T\Gamma R^{-1}\dot{\mu}k \le \|SA_mB_m\|\,\|\sigma\|^2 + k_1\|S\|\,\|B_m\|\,\|\sigma\|^2 \\
&\quad + \|SA_mT\|\,\|\sigma\|\eta(t) + k_1\|S\|\,\|T\|\,\|\sigma\|\eta(t) + \{k_2 + k_3[\|T\|\eta(t) \\
&\quad + \|B_m\|\,\|\sigma\|]\}\|\sigma\| - [\|SA_mB_m\| + \hat{k}_1\|S\|\,\|B_m\| \\
&\quad + \hat{k}_3\|B_m\|]\|\sigma\|^2 - [\|SA_mT\| + \hat{k}_1\|S\|\,\|T\| + \hat{k}_3\|T\|]\|\sigma\|\eta(t) \\
&\quad - \hat{k}_2\|\sigma\| - \alpha\|\sigma\| + \bar{k}^T\Gamma\dot{\bar{k}} + k^T\Gamma R^{-1}\dot{\mu}k \\
&\quad \le -\alpha\|\sigma\| + \bar{k}_1\|S\|\,\|\sigma\|[\|B_m\|\,\|\sigma\| + \|T\|\eta(t)] + \bar{k}_2\|\sigma\| \\
&\quad + \bar{k}_3\|\sigma\|[\|B_m\|\,\|\sigma\| + \|T\|\eta(t)] + \bar{k}^T\Gamma\dot{\bar{k}} + k^T\Gamma R^{-1}\dot{\mu}k
\end{aligned} \tag{46}$$

Using the fact $\dot{\bar{k}}_i = -\dot{\hat{k}}_i$ $(i = 1, 2, 3)$ and $\dot{\mu}k = -R^{-1}(\mu k)$, then

$$\dot{\tilde{V}} \le -\alpha\|\sigma\| + \bar{k}^T\Gamma(\mu\hat{k}) - k^T\Gamma R^{-1}(\mu k) = -\alpha\|\sigma\| + \Xi \tag{47}$$

Here, $\Xi = \bar{k}^T\Gamma(\mu\hat{k}) - k^T\Gamma R^{-1}(\mu k) = \sum_{i=1}^{3}(\bar{k}_i p_i\mu_i\hat{k}_i - k_i^2 p_i\mu_i)$ $(i = 1, 2, 3)$, where

$$\begin{aligned}
&\bar{k}_i p_i\mu_i\hat{k}_i - k_i^2 p_i\mu_i = p_i\mu_i[(k_i - \hat{k}_i)\hat{k}_i - k_i^2] = p_i\mu_i[k_i\hat{k}_i - \hat{k}_i^2 \\
&\quad - k_i^2] < p_i\mu_i\left[\left(\frac{k_i^2 + \hat{k}_i^2}{2}\right) - \hat{k}_i^2 - k_i^2\right] = -p_i\mu_i\left(\frac{k_i^2 + \hat{k}_i^2}{2}\right) < 0
\end{aligned} \tag{48}$$

So we can also obtain the following inequality:

$$\dot{\tilde{V}} \le -\alpha\|\sigma\| = -g(t) \le 0 \tag{49}$$

where $g(t) = \alpha\|\sigma\|$. Integrating the above equation from zero to t yields

$$\tilde{V}(0) \ge \tilde{V}(t) + \int_0^t g(\tau)\,\mathrm{d}\tau \ge \int_0^t g(\tau)\,\mathrm{d}\tau \quad \forall\ t \ge 0 \tag{50}$$

As time t goes to infinity, the above integral is always less than or equal to $\tilde{V}(0)$. However, $\tilde{V}(0)$ is finite and positive, then we have $g(t) \to 0$ as $t \to \infty$ from Lemma 3; that is

$$\lim_{t\to\infty} g(t) = \lim_{t\to\infty}\alpha\|\sigma\| = 0 \tag{51}$$

Equation (51) guarantees that $S(t) \to 0$ as t goes to infinity. Then the proof is completed.

V. Simulation Results

To demonstrate the effectiveness of the proposed control schemes, numerical simulations have been performed and presented in this section. The key technical indexes of flexible spacecraft used in the simulation are given in [12]. In this work, the reference model is the normal system with the first two low-order modes of five, $\omega_{1m} = 3.161$ rad/s and $\omega_{2m} = 16.954$ rad/s, and the damping ratio $\xi_{1m} = \xi_{2m} = 0.001$, respectively, while for the actual spacecraft model, five flexible modes are considered in the simulation. Furthermore, the relations between the parametric uncertainty, the actual natural frequencies ω_i, and the normal natural frequencies ω_{im}, can be expressed as follows:

$$|\omega_i^2 - \omega_{im}^2| \le \delta_A\omega_{im}^2, \qquad (i = 1, 2) \tag{52}$$

where $\delta_A = 0.2$. Assume $\Delta B = B_m \cdot 0.5\sin(4t)$, and the uncertainty input, $D_B = 0.1$, is less than the upper bound of input variation, $\delta_B = 1$, and the external disturbance $d(t)$ is a random disturbance torque, given by

$$d(t) = d_{\max}N(\bullet) \tag{53}$$

whose maximum absolute $d_{\max}$ has been fixed to 0.1 Nm; $N(\bullet)$ denotes the normal distribution with mean zero and standard deviation one.

In this simulation, the flexible spacecraft is commanded to perform a 60-deg slew. The main control objective of the flexible spacecraft is to aim the precision pointing within a certain 0.002 deg error in a short time period, the desired motion of the rigid body not beyond 0.002 deg/s and during the entire slewing motion, the vibrations being less stirred with the maximum amplitude of the vibration no more than 0.1 $\mathrm{kg}^{1/2}$ m (note that the units here are not meters, simply because of our choice of vibration mode coordinates). Here, the vibration energy level is described by $E = \dot{q}^T\dot{q} + q^T K_{qq} q$.

For comparison, three cases are conducted: 1) attitude maneuver control using only PD controllers and PD control + input shaping (IS); 2) attitude maneuver control using the conventional variable structure output feedback control (CVSOFC) given in [26], and also CVSOFC + IS; 3) attitude maneuver control using only proposed dynamic variable or adaptive variable structure output feedback controllers (36) or (41) with the adaptive law (43), and the proposed DVSOFC or (DAVSOFC) + IS. In the simulation, the input shaper is the convolved four impulses zero vibration derivative–derivative (ZVDD) shaper for the first mode and two impulses zero vibration ZV shaper for the second mode. All computations and plots shown in the paper were performed using the MATLAB/Simulink software package.

A. PD Control and PD + IS

To demonstrate the performance of the vibration control schemes, a PD feedback control of collocated sensor signals is adopted for control of rigid body motion of the spacecraft A block diagram of the PD controller is shown in Fig. 4, where K_p and K_v are the proportional and derivative gains, respectively, θ represents the hub angle, $\dot{\theta}$ represents hub velocity, and θ_d is the reference hub angle. Essentially, the task of this controller is to maneuver the flexible spacecraft to the specified angle of demand. The hub angle and hub velocity signals are fed back and used to control the hub angle for the spacecraft.

In this study, a root locus approach is used to design the PD controller. The proportional gain and the derivative gain of the PD controller for attitude control are 15 and 50, respectively. The corresponding hub angle and velocity of the spacecraft, modal vibrations, and the required control torque of response using the PD control are shown in Fig. 5. From Fig. 5, no acceptable hub angle and velocity responses were achieved with nearly 0.05 deg steady error and 0.05 deg/s rate error. Moreover, a significant amount of vibration occurred during the maneuvering of the flexible spacecraft as demonstrated in the vibration energy's plot of Fig. 5, with more than 1.4 $kg^{1/2}$ m in energy.

To actively suppress the modal vibration, a hybrid control structure for control of rigid body motion and vibration suppression of the flexible appendages using PD control with active vibration reduction technique based on shaping is presented here. A block diagram of the hybrid control scheme is shown in Fig. 6. In this case, the PD controller parameters for the attitude control remain the same

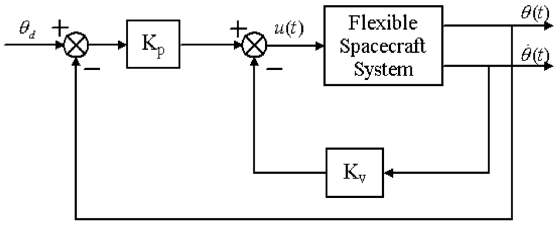

Fig. 4 The PD control structure.

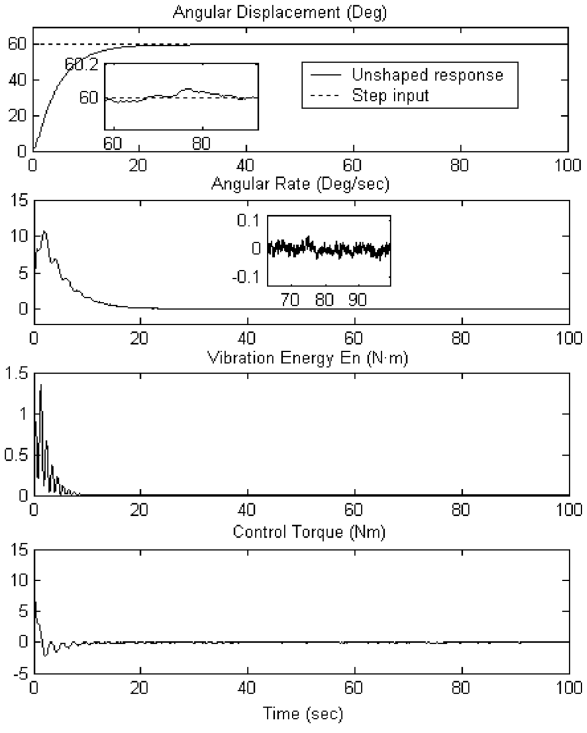

Fig. 5 Time response for using the PD control case.

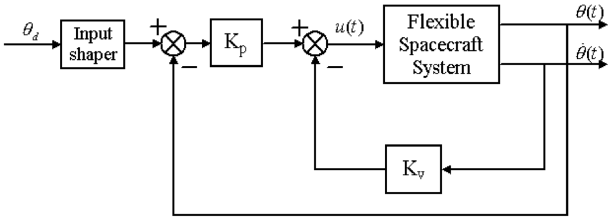

Fig. 6 PD with input shaper structure.

for a fair comparison, and a four impulses ZVDD shaper for the first mode and a two impulses ZV shaper for the second mode are implemented. Figure 7 shows the results of employing the PD controller with input shaper. It is clear from the top plot of Fig. 7 that the pointing accuracy was improved with less than 0.01 deg and the stability accuracy was less than 0.02 deg/s. Moreover, the relatively large amplitude vibrations excited by rapid maneuvers can be actively suppressed, and the energy is less than 0.1 $kg^{1/2}$ m, as shown in the third plot from the top of Fig. 7. This reflects the effectiveness of the input shaping for active vibrations suppression. However, for the PD control or PD + IS case, the above control objective mentioned cannot be achieved; despite the fact that there still exists some room for improvement with different design parameter sets (K_p, K_d), there is not much improvement in the hub-angle and velocity responses.

B. CVSOFC and CVSOFC + IS

For the purpose of comparison, the system employed by the VSOFC presented in [26] is also considered in this section. The same simulation case is repeated with the traditional VSOFC replacing the PD control for a fair complexion and the results of simulation were shown in Fig. 8. For this case, the vibration can be successfully suppressed and the vibration energy is no more than 0.06 $kg^{1/2}$ m, but the angle and velocity response cannot satisfy the requirements of the control objective with 0.005 deg and 0.005 deg/s for steady and rate error, respectively. To further improve the performance of the system, the convolved first-mode-ZVDD shaper and second-mode-ZV shaper is also used. The plots of this case are shown in Fig. 9. In this case, even though the vibration observed in Fig. 9 can be reduced

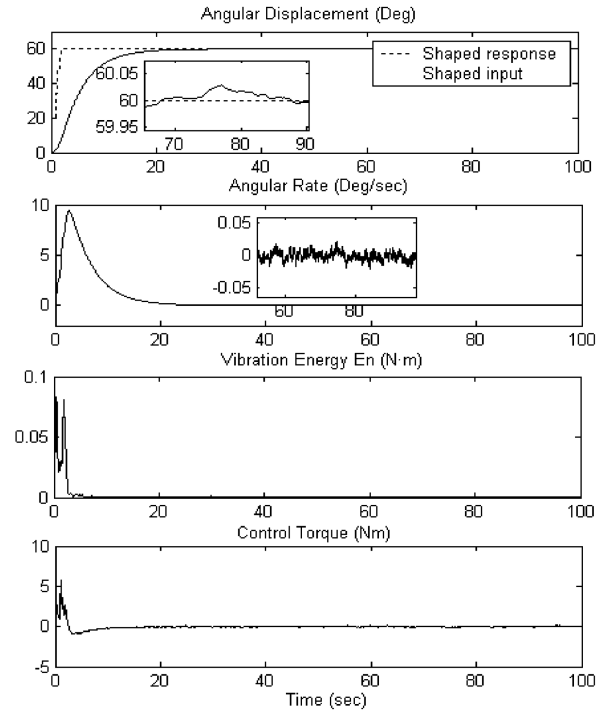

Fig. 7 Time response of using the PD + IS technique case.

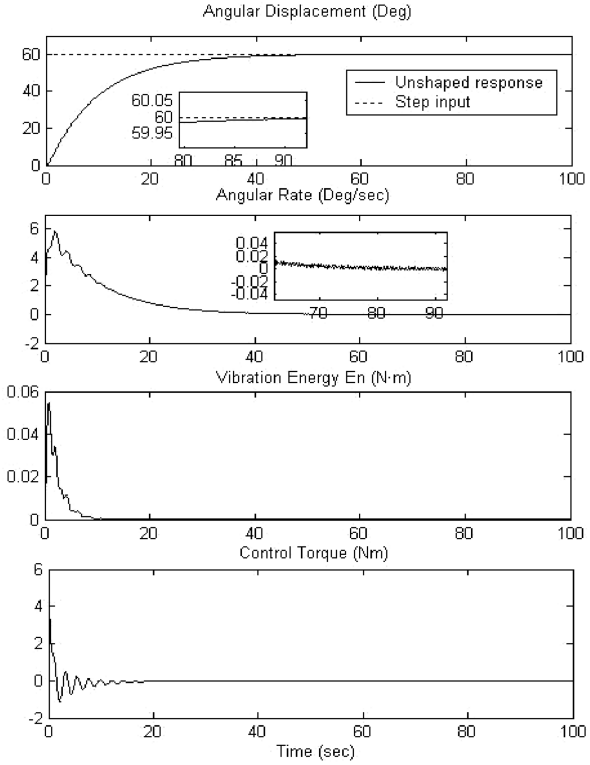

Fig. 8 Time response of using CVSOFC with case.

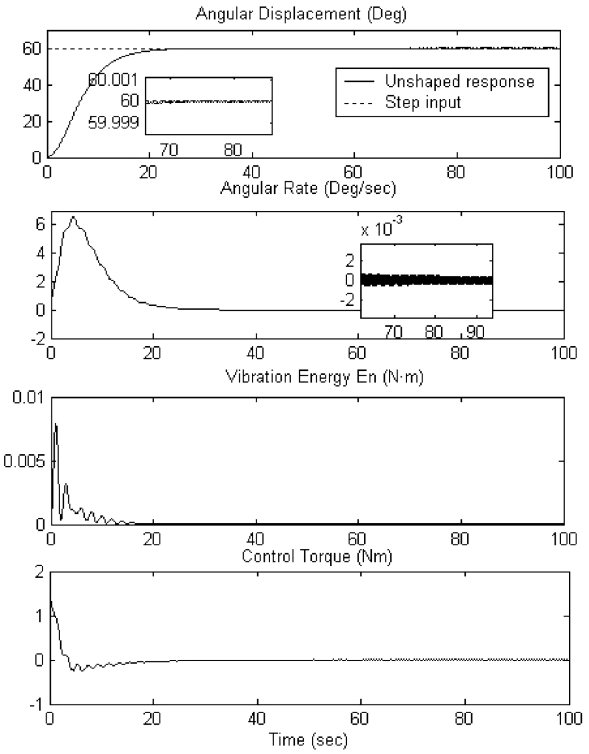

Fig. 10 Time response of using proposed DVSOFC case.

further with less than 0.006 $kg^{1/2}$ m, the pointing accuracy and stability of spacecraft cannot satisfy the requirement yet.

C. DVSOFC and DVSOFC + IS

Figure 10 shows the results of implementing only the proposed sliding mode output feedback controller acting on the rigid hub in the presence of mismatched uncertainty. From the top plot of Fig. 10, the imposed desired angular displacement is accurately achieved by employing the DVSOFC law. From the comparison of Figs. 5, 8, and 10, it is clear that the relatively large amplitude vibrations excited by rapid maneuvers can be passively suppressed, and the angle and velocity responses do satisfy the requirements of the control objective with less than 0.001 deg and 0.0002 deg /s, respectively.

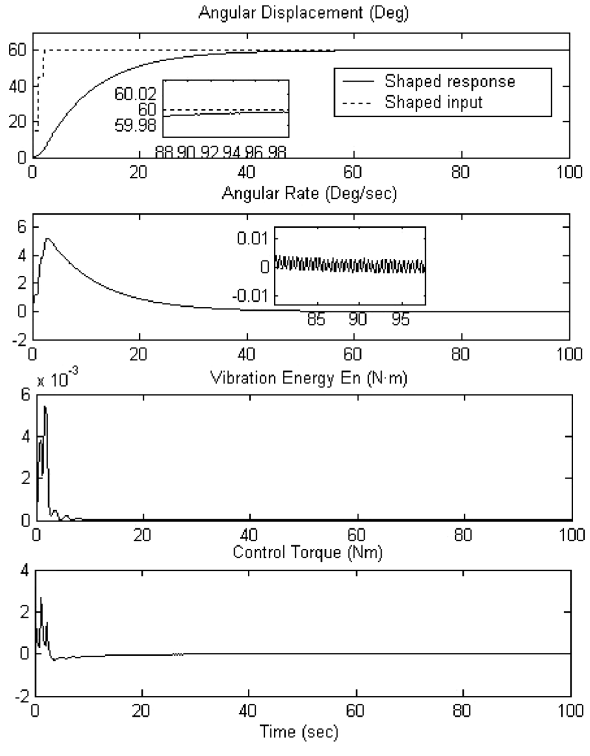

Fig. 9 Time response of using CVSOFC + IS with case.

Even though the sliding mode controller can suppress the relatively large amplitude vibrations induced by rapid maneuvers, some residual microvibrations may be present. To further improve the performance of the system, the combined DVSOFC + IS is also employed. In this case, the DVSOFC parameters for the attitude control remain the same for a fair comparison, and four impulses ZVDD shaper for the first mode and two impulses ZV shaper for the second mode are also implemented. Figure 11 shows the results of employing this combination. The imposed desired angular displacement is accurately achieved and the relatively large amplitude vibrations excited by rapid maneuvers can be actively further suppressed, as shown in the third plot from the top of Fig. 11. This further demonstrates the validity of an active vibration reduction base on the input-shaping technique.

For the adaptive control case in Eq. (41) with adaptive law (43), the same tests are also repeated with the same control parameters and the simulation results are shown in Figs. 12–14. In this case, for the adaptive gain $\hat{k}_i$ and the term μ_i, the initial values are arbitrarily chosen; that is $\hat{k}_{i0} = 0$ and $\mu_i(0) = 0.05$, and the adaptive gains $p_i = 0.01$ are chosen. With the effect of the negative feedback term, the estimates of $\hat{k}_i$ are bounded as shown in Fig. 14. It should be pointed out that without the feedback term $-\mu_i \hat{k}_i$, the estimated gains $\hat{k}_i$ become unbounded since the restriction to the sliding surface cannot always be achieved, which will deteriorate the stability of the system. For this case, the response of attitude, angular velocity, and the modal vibration energy are not shown because of space limitation. It is clear that, from the comparison of the cases using DVSOFC and ADVSOFC (adaptive DVSOFC), the vibration energy in the latter case is less than the first and the control torque magnitude is also reduced. In addition, the latter case also generates smoother control action than the former. The same results can also be concluded from the input-shaping integrated cases. This reflects the advantages of ADVSOFC over the DVSOFC case, but this is achieved at the expense of greater complexity and the requirement

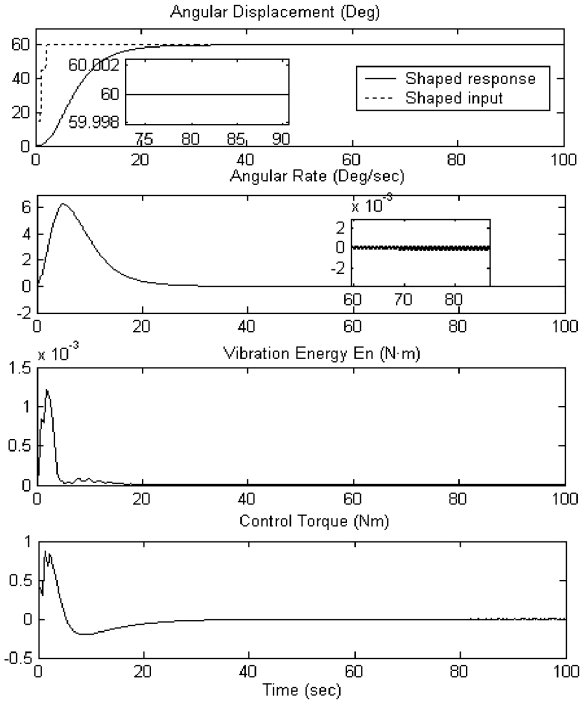

Fig. 11 Time response of using proposed DVSOFC + IS case.

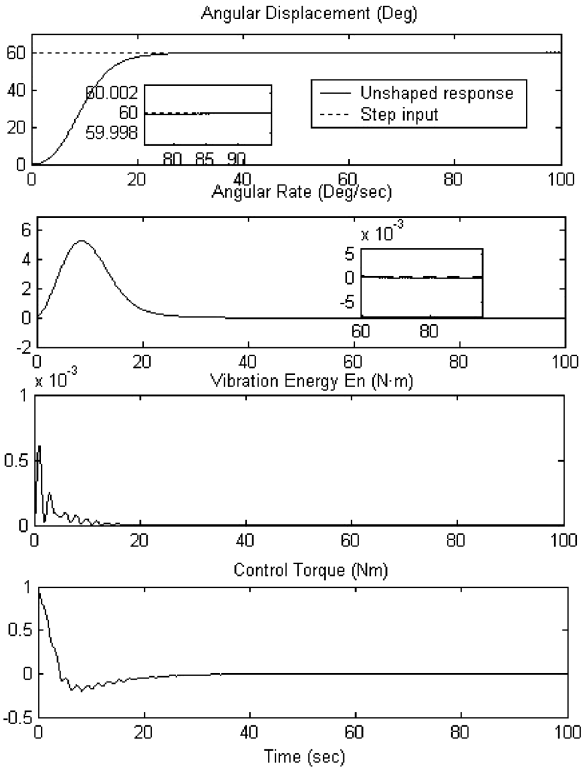

Fig. 12 Time response of using proposed ADVSOFC case.

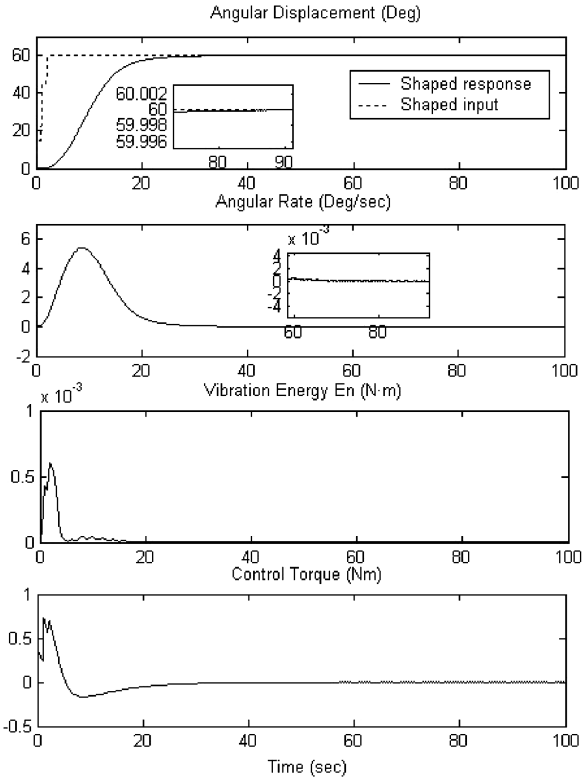

Fig. 13 Time response of using proposed ADVSOFC + IS with smoothed control case.

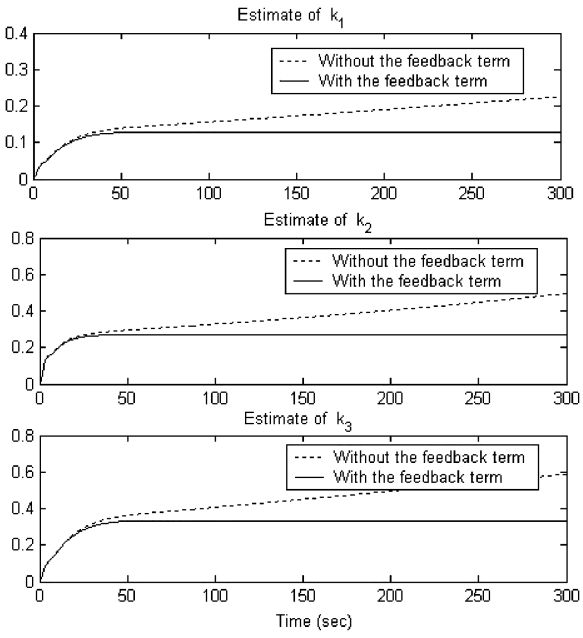

Fig. 14 Time response of estimate of gain k_i ($i = 1, 2, 3$).

that the parameters for the adaptive control law in (43) must be chosen properly. In addition, when ±20% errors of the natural frequency ω_1 and ω_2 are also considered in the simulation, the same trends as Figs. 11–14 were also found (figures not shown because of space limitation).

From the comparison of the previous cases, it is shown that the proposed approach can not only accomplish the attitude control during maneuvers, but also simultaneously suppresses the undesired vibrations of the flexible appendages. Furthermore, the information of the upper bound of the perturbations and uncertainty is not required beforehand when the adaptive version of the developed variable structure output feedback control is adopted. For the several different control cases, the overall results on settling time, peak vibration energy, pointing accuracy, and stability accuracy are also summarized in Table 1.

VI. Conclusions

In this paper, a new approach for vibration reduction of flexible spacecraft during attitude maneuver operations is presented. This

Table 1 Performance comparison on settling time, peak vibration energy, pointing accuracy, and stability accuracy

	Settling time, s	Peak vibration energy, $kg^{1/2}$ m	Pointing accuracy, deg	Stability accuracy, deg/s
PD	30	1.4	0.05	0.05
PD + IS	32	0.8	0.01	0.05
CVSOFC	49	0.055	0.005	0.005
CVSOFC + IS	55	0.0058	0.004	0.0004
DVSOFC	23	0.07	<0.002	<0.0002
DVSOFC + IS	32	0.0012	<0.002	<0.0002
ADVSOFC	26	0.0006	<0.002	<0.002
ADVSOFC + IS	33	0.0006	<0.002	<0.002

approach integrates the method of command input shaping and the theory of variable structure output feedback control that takes into account parameter uncertainties and external disturbances, provided that the bounds are known. The method of command input shaping is implemented outside of the feedback loop to modify the existing command so that less vibration will be caused by the command itself. The amplitudes and instances of the impulses application are obtained for the natural frequency and damping ratio of the reference model (normal plant), respectively, such that the exact elimination of the residual vibration is achieved for the reference model. Because measurement of elastic modes is, generally, not available in practice, synthesis of the attitude controller using only the attitude and angular rate information fed back are considered. The controller based on a dynamic variable structure output feedback control is designed to make the closed-loop system behave like the reference system with input shaper and suppress the vibration of the flexible structures in the presence of parametric uncertainty and external disturbances. In this case, this is an effective method of implementing input shaping for satisfactory performance and robustness even when parameter variations and external disturbances occur simultaneously in the process. In addition, an adaptive version of this algorithm is also proposed, which removes the disadvantages of the variable structure controller, and can result in precise response to attitude control command and effective suppression to the vibration of its flexible appendages in the presence of disturbances and mismatched uncertainty. Simulation results of a slew operation of a spacecraft with flexible appendage demonstrate that the proposed technique can significantly reduce the vibration of the flexible beam during slew operations.

Acknowledgements

The authors wish to thank the anonymous reviewers and Associate Editor Wodek Gawronski for valuable comments and suggestions that helped improve the presentation of this paper.

References

[1] Singer, N., and Seering, W., "Preshaping Command Inputs to Reduce System Vibration," *Journal of Dynamic Systems, Measurement, and Control*, Vol. 112, No. 1, 1990, pp. 76–82.

[2] Singh, T., and Heppler, G. R., "Shaped Input Control of a System with Multiple Modes," *Journal of Dynamic Systems, Measurement, and Control*, Vol. 115, No. 3, 1993, pp. 341–347.

[3] Singhose, W., Banerjee, A., and Seering, W., "Slewing Flexible Spacecraft with Deflection-Limiting Input shaping," *Journal of Guidance, Control, and Dynamics*, Vol. 20, No. 2, 1997, pp. 291–298.

[4] Banerjee, A., and Singhose, W., "Command Shaping for Nonlinear Tracking Control of a Two-link Flexible Manipulator," *Proceedings of the 1997 AAS/AIAA Astrodynamics Conference*, Vol. 97, No. 2, 1997, pp. 1856–1876.

[5] Hillsley, K., and Yurkovich, L. S., "Vibration Control of a Two-Link Flexible Robot Arm," *Dynamics and Control*, Vol. 3, No. 3, 1993, pp. 261–280.

[6] Hillsley, K., and Yurkovich, S., "Vibration Control of a Two-Link Flexible Robot Arm," *IEEE International Conference on Robotics and Automation*, IEEE Comput. Soc. Press, Los Alamitos, CA, Vol. 3, 1991, pp. 212–216.

[7] Song, G., Buck, N., and Agrawal, B., "Spacecraft Vibration Reduction Using Pulse-Width Pulse-Frequency Modulated Input Shaper," *Journal of Guidance, Control, and Dynamics*, Vol. 22, No. 3, 1999, pp. 433–440.

[8] Shan, J. J., Liu, H. T., and Sun, D., "Modified Input Shaping for a Rotation Single-Link Flexible Manipulator," *Journal of Sound and Vibration*, Vol. 285, No. 1-2, 2005, pp. 187–207.

[9] Gorinevsky, D., and Vukovich, G. "Nonlinear Input Shaping Control of Flexible Spacecraft Reorientation Maneuver," *Journal of Guidance, Control, and Dynamics*, Vol. 21, No. 2, 1998, pp. 264–270.

[10] Craig, F. C., and Lucy Y. P., "Adaptive Input Shaping for Maneuvering Flexible Structures," *Automatica*, Vol. 40, No. 4, 2004, pp. 685–693.

[11] Romano, M., Agrawal, B., and Bernelli, Z. F., "Experiments on Command Shaping Control of a Manipulator with Flexible Links," *Journal of Guidance, Control, and Dynamics*, Vol. 25, No. 2, 2002, pp. 232–239.

[12] Hu, Q. L., and Ma, G. F., "Vibration Suppression of Flexible Spacecraft During Attitude Maneuvers," *Journal of Guidance, Control, and Dynamics*, Vol. 28, No. 2, 2005, pp. 377–380.

[13] Shan, J. J., Sun, D., and Liu, D., "Design for Robust Component Synthesis Vibration Suppression of Flexible Structures with On-off Actuators," *IEEE Transactions on Robotics and Automation*, Vol. 20, No. 3, 2004, pp. 512–525.

[14] Fanson, J. L., and Caughey, T. K., "Positive Position Feedback Control for Large Structure," *AIAA Journal*, Vol. 28, No. 4, 1990, pp. 717–724.

[15] Utkin, V. I., "Variable Structure Systems with Sliding Modes," *IEEE Transactions on Automatic Control*, Vol. 22, No. 2, 1977, pp. 212–222.

[16] Hung, J. Y., Gao, W., and Hung, J. C., "Variable Structure Control: A Survey," *IEEE Transactions on Industrial Electronics*, Vol. 40, No. 1, 1993, pp. 2–22.

[17] Yong, K., Utkin, V., and Ozguner, U., "A Control Engineer's Guide to Sliding Mode Control," *IEEE Transactions on Control Systems Technology*, Vol. 7, No. 3, 1999, pp. 328–342.

[18] Crassidis, J. L., and Markley, F. L., "Sliding Mode Control Using Modified Rodrigues Parameters," *Journal of Guidance, Control, and Dynamics*, Vol. 19, No. 6, 1996, pp. 1381–1383.

[19] Iyer, A., and Singh, S., "Variable Structure Slewing Control and Vibration Damping of Flexible Spacecraft," *Acta Astronautica*, Vol. 25, No. 1, 1991, pp. 1–9.

[20] Lo, S., and Chen, Y., "Smooth Sliding Mode Control for Spacecraft Attitude Tracking Maneuvers," *Journal of Guidance, Control, and Dynamics*, Vol. 18, No. 6, 1995, pp. 1345–1349.

[21] Dwyer, T. A. W., III, and Sira-Ramirez, H., "Variable Structure Control of Spacecraft Attitude Maneuver," *Journal of Guidance, Control, and Dynamics*, Vol. 11, No. 3, 1988, pp. 262–270.

[22] Öz, H., and Mostafa, O., "Variable Structure Control System (VSCS) Maneuvering of Flexible Spacecraft," *Journal of the Astronautical Sciences*, Vol. 36, No. 3, 1988, pp. 311–344.

[23] Singh, S. N., "Robust Nonlinear Attitude Control of Flexible Spacecraft," *IEEE Transactions on Aerospace and Electronic Systems*, Vol. 23, No. 3, 1987, pp. 380–387.

[24] Heck, B. S., and Ferri, A. A., "Application of Output Feedback to Variable Structure Systems," *Journal of Guidance, Control, and Dynamics*, Vol. 12, No. 6, 1989, pp. 932–935.

[25] Zak, S. H., and Hui, S., "On Variable Structure Output Feedback Controllers for Uncertain Dynamic Systems," *IEEE Transactions on Automatic Control*, Vol. 38, No. 10, 1993, pp. 1509–1512.

[26] Yallapragada, S. V., Heck, B. S., and Finney, J. D., "Reaching Conditions for Variable Structure Control with Output Feedback," *Journal of Guidance, Control, and Dynamics*, Vol. 19, No. 4, 1996, pp. 848–853.

[27] Wang, W. J., and Fan, Y. T., "New Output Feedback Design in Variable Structure Systems," *Journal of Guidance, Control, and Dynamics*, Vol. 17, No. 2, 1994, pp. 337–340.

[28] Kwan, C. M., "Sliding Control Using Output Feedback," *Journal of Guidance, Control, and Dynamics*, Vol. 19, No. 3, 1996, pp. 731–733.
[29] Kwan, C. M., "Further Results on Variable Output Feedback Controllers," *IEEE Transactions on Automatic Control*, Vol. 46, No. 9, 2001, pp. 1505–1508.
[30] Lewis, A. S., and Sinha, A., "Sliding Mode Control of Mechanical Systems with Bounded Disturbance via Output Feedback," *Journal of Guidance, Control, and Dynamics*, Vol. 22, No. 2, 1999, pp. 235–240.
[31] Lewis, A. S., "Robust Output Feedback Using Sliding Mode Control," *Journal of Guidance, Control, and Dynamics*, Vol. 24, No. 5, 2001, pp. 873–878.
[32] Shyu, K. K., Tsai, Y. W., and Lai, C. K., "A Dynamic Output Controllers for Mismatched Uncertain Variable Structure Systems," *Automatica*, Vol. 37, No. 5, 2001, pp. 775–779.
[33] Wheeler, G., Su, C. Y., and Stepanenko, Y., "A Sliding Mode Controller with Improved Adaptation Laws for the Upper Bounds on the Norm of Uncertainties," *Automatica*, Vol. 34, No. 12, 1998, pp. 1657–1661.
[34] Yoo, D. S., and Chung, M. J., "A Variable Structure Control with Simple Adaptation Laws for Upper Bounds on the Norm of the Uncertainties," *IEEE Transactions on Automatic Control*, Vol. 37, No. 6, 1992, pp. 159–165.
[35] Hsu, K. C., "Adaptive Variable Structure Control Design for Uncertain Time-Delayed Systems with Nonlinear Input," *Dynamics and Control*, Vol. 8, No. 4, 1998, pp. 341–354.
[36] Turner, J. D., and Chun, H. M., "Optimal Distributed Control of a Flexible Spacecraft During a Large-Angle Maneuver," *Journal of Guidance, Control, and Dynamics*, Vol. 7, No. 3, 1984, pp. 257–264.
[37] Karray, K., Grewal, A., Glaum, M., and Modi, V., "Stiffening Control of a Class of Nonlinear affine System," *IEEE Transactions on Aerospace and Electronic Systems*, Vol. 33, No. 2, 1997, pp. 473–484.
[38] Hu, Q. L., and Liu, Y. Q. "A Hybrid Scheme of Feed-Forward/ Feedback Control for Vibration Suppression of Flexible Spacecraft with On-Off Actuators During Attitude Maneuver," *International Journal of Information Technology*, Vol. 11, No. 12, 2005, pp. 95–107.
[39] Slotine, J., and Li, W., *Applied Nonlinear Control*, Prentice–Hall, Upper Saddle River, NJ, 1991.